The Journal of Neuroscience, July 15, 2000, *20*(14):5483–5495

The Midbrain Precommand Nucleus of the Mormyrid Electromotor Network

Gerhard von der Emde,[1] Leonel Gómez Sena,[2,3] Rafaella Niso,[2] and Kirsty Grant[2]

[1]Institut für Zoologie, Universität Bonn, Poppelsdorfer Schloss, 53115 Bonn, Germany, [2]Unité des Neurosciences Intégratives et Computationnelles, Institut de Neurobiologie Alfred Fessard, Centre National de la Recherche Scientifique, 91198 Gif-sur-Yvette, Cedex, France, and [3]Department of Biomathematics, Faculty of Science, University of the Republic, Montevideo, Uruguay

The functional role of the midbrain precommand nucleus (PCN) of the electromotor system was explored in the weakly electric mormyrid fish *Gnathonemus petersii*, using extracellular recording of field potentials, single unit activity, and microstimulation *in vivo*.

Electromotor-related field potentials in PCN are linked in a one-to-one manner and with a fixed time relationship to the electric organ discharge (EOD) command cycle, but occur later than EOD command activity in the medulla. It is suggested that PCN electromotor-related field potentials arise from two sources: (1) antidromically, by backpropagation across electrotonic synapses between PCN axons and command nucleus neurons, and (2) as corollary discharge-driven feedback arriving from the command nucleus indirectly, via multisynaptic pathways.

PCN neurons can be activated by electrosensory input, but this does not necessarily activate the whole motor command chain. Microstimulation of PCN modulates the endogenous pattern of electromotor command in a way that can mimic the structure of certain stereotyped behavioral patterns. PCN activity is regulated, and to a certain extent synchronized, by corollary discharge feedback inhibition. However, PCN does not generally function as a synchronized pacemaker driving the electromotor command chain. We propose that PCN neurons integrate information of various origins and individually relay this to the command nucleus in the medulla. Some may also have intrinsic, although normally nonsynchronized, pacemaker properties. This descending activity, integrated in the electromotor command nucleus, will play an important modulatory role in the central pattern generator decision process.

Key words: electric fish; motor command; pacemaker; corollary discharge; central pattern generator; mormyrid; premotor pathways; sensory motor integration

Rhythmic motor behaviors are part of the behavioral inventory of most vertebrates. Examples include locomotor activity, rhythmic vocalizations, electromotor behaviors of weakly electric fish, and microsaccadic eye movements. Many of these behaviors have similar physiological properties and may have developed according to common ontogenetic and phylogenetic principles (Grillner and Georgopoulos, 1996; Bass and Baker, 1997). These behaviors are repetitive, more or less stereotyped, and have a temporal pattern that is produced by brain areas referred to as central pattern generators, neural oscillators, or pacemakers (Grillner et al., 1995; Katz, 1995; Cohen et al., 1996; Grant et al., 1999). Pacemaker networks produce a basic temporal rhythm of behavior, which in turn can be modified to various degrees by premotor centers. In this paper, we investigate the physiology of the midbrain precommand nucleus (PCN) of the electromotor system in the weakly electric mormyrid fish *Gnathonemus petersii*, and its role in the modulation of the intrinsic rhythm of electromotor behavior.

The all-or-none, pulse-type electric organ discharge (EOD) in mormyrid fish is driven by an irregularly rhythmic central command network. Electroemission is used for active electrolocation (Lissmann and Machin, 1958; von der Emde, 1999) and intraspecific electrocommunication (Hopkins, 1988; Kramer, 1990). EOD displays reveal a structured temporal organization (Teyssedre et al., 1987), including endogenously controlled regularization, phase-locking to external EOD signals, and sensorimotor reflexes. Distinct electromotor behaviors are associated with exploration or social interactions (Bauer and Kramer, 1974; Bell et al., 1974; Toerring and Moller, 1984; Moller et al., 1989; Serrier and Moller, 1989). Similar EOD patterns can also be elicited experimentally by artificial electric stimuli (Moller, 1970; Bauer, 1974; Serrier, 1982).

Spinal electromotoneurons driving the electric organ receive a descending command from a central pattern generator in the medulla. This consists of two adjacent midline nuclei, the command nucleus (CN), which initiates the electromotor commands, and the medullary relay nucleus (MRN), whose function is to synchronize the descending command volley (Szabo, 1957; Aljure, 1964; Bennett et al., 1967; Bell et al., 1983; Elekes et al., 1985; Elekes and Szabo, 1985; Grant et al., 1986, 1999). The endogenous rhythm of the electromotor command depends on the membrane properties of the CN neurons and on their postsynaptic integration of afferent activity (Grant et al., 1986).

The afferent and efferent connections of the medullary relay and command nuclei were established by tracing using horseradish peroxidase (Bell et al., 1983). In addition to the descending electromotor command pathway, these authors identified an ascending corollary discharge pathway projecting from the command nucleus, via the bulbar command-associated nucleus (BCA) to the mesencephalic command-associated nucleus (MCA). The bilateral PCN situated at the mesencephalic–diencephalic border (Bell et al., 1983) (Fig. 1*A*) was identified as the principal source of descending afferent projections to CN.

The aim of the present study was to identify the precommand nucleus electrophysiologically and to explore its functional role in electromotor command generation.

Received Dec. 27, 1999; revised April 20, 2000; accepted April 27, 2000.

This work was supported by the French Centre National de la Recherche Scientifique, the Deutsche Forschungsgemeinschaft (Em 43/4-1; Em 43/1-3), a Franco-Italian exchange fellowship to R.N., a Franco-Uruguayan exchange fellowship to L.G., European Commission contract number CI1*CT92 0085 to K.G., and the Franco-German and Franco-Uruguayan exchange programs PROCOPE (K.G. and G.v.d.E.) and ECOS (K.G. and L.G.). Some of the experiments were conducted by G.v.d.E. at the Scripps Institute of Oceanography (La Jolla, CA) in receipt of financial support from grants made to the late Walter Heiligenberg. We are indebted to Dr. T. H. Bullock for his support and encouragement, Drs. C. Wong and J. Serrier for their practical help in many respects, and Drs. C. Bell and H. Bleckmann for valuable discussion and constructive criticism of this manuscript.

Correspondence should be addressed to Dr. Kirsty Grant, Unité de Neurosciences Intégratives et Computationnelles, Institut de Neurobiologie Alfred Fessard, Centre National de la Recherche Scientifique 1, Avenue de la Terrasse, F-91198 Gif-sur-Yvette, Cedex, France. E-mail: grant@iaf.cnrs-gif.fr.

 0270-6474/00/205483-13$15.00/0

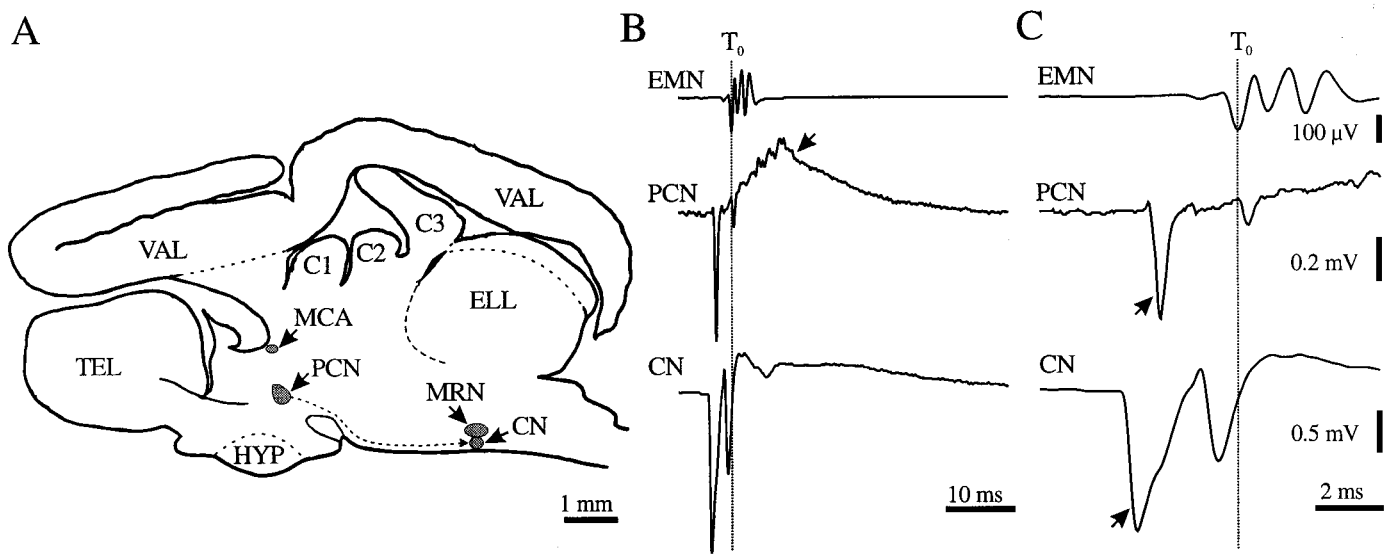

Figure 1. Electromotor-related field potentials in PCN. *A,* Schematic diagram of *Gnathonemus petersii* brain in sagittal section, showing relative positions of the PCN, the CN, the MRN, and the MCA (CN and MRN are midline nuclei; PCN and MCA are bilateral nuclei, actually situated in a more lateral parasagittal plane). *C1, C2, C3,* Cerebellar lobes; *ELL,* electrosensory lateral line lobe; *HYP,* hypothalamus; *TEL,* telencephalon; *VAL,* valvula cerebelli. *B, C, Top traces,* EMN recorded at the skin surface above the electric organ; *middle* and *bottom traces,* electromotor-related field potentials recorded extracellularly in the PCN and CN, in the same fish (averaged traces: EMN, $n = 50$; PCN, $n = 50$; CN, $n = 80$). T_0 defines the first negative peak of the EMN volley which, by convention, is used as the temporal reference point used to compare the timing of field potentials and unit activity in this and other figures. The much smaller negative wave preceding T_0 corresponds to the descending afferent volley. The center of PCN was reliably identified by the slow positive potential (*B, arrow, middle trace*) that follows the two initial negative peaks. *C,* The relative timing of the negative field potentials in PCN and CN (*arrows*): note that electromotor-related field potentials began 0.7 msec earlier in CN (*bottom trace*) than in PCN (*middle trace*).

MATERIALS AND METHODS

Animals. Thirty *Gnathonemus petersii*, ranging in length from 8.0 to 13.8 cm were used in this study. All fish were acquired from registered fish dealers in either Germany or the United States.

Preparation. Fish were anesthetized initially in tricaine methylsulfonate solution (MS-222; Sandoz, Basel, Switzerland or Sigma, St. Louis, MO; concentration 1:10,000). Anesthesia was maintained afterward by buccal perfusion of aerated MS-222 solution (concentration, 1:30,000; flow rate, 50 ml/min). For surgery the fish was supported laterally against a wax block or in a foam-lined support clamp, with only the dorsal surface of the head above the water. Under additional local anesthesia (2% lidocaine gel), a small opening was made in the cranium above the midbrain (for recording from PCN) or above the hindbrain (for recording from CN), exposing part of the valvula cerebelli, which covers the whole dorsal brain of *G. petersii*. At the end of surgery all wound edges were again treated with lidocaine gel. The fish was paralyzed by intramuscular injection of either gallamine triethiodide (Flaxedil Spécia; 0.5 mg) or D-tubocurarine (Sigma; 0.075 mg). MS-222 anesthesia, which suppresses electromotor command activity, was discontinued, and artificial respiration was maintained by a perfusion of aerated aquarium water.

The discharge of the electric organ is blocked by curarization, but the descending command signal, in the form of the synchronized three-spike spinal electromotoneuron volley (EMN) (Fig. 1*B,C*), can still be recorded using two silver ball electrodes placed on the skin over the electric organ, relayed to a high gain differential amplifier. The first large negative peak of the electromotoneuron volley has been defined as a "zero" time reference (Fig. 1*B,C,* T_0) to normalize records from different fish. In the noncurarized fish, an EOD would normally occur 4.5 msec after T_0.

Recording and stimulation in PCN. PCN was localized with a single-barrel glass micropipette (tip diameter, 1–3 μm) filled with 3 M NaCl. Electromotor command-related field potentials and extracellular single-unit responses were recorded either with a World Precision Instruments (WPI) M-707A electrometer or a WPI DAM 80 differential amplifier, digitized (Sony digital audio processor; PCM 1300) and recorded on a videotape system for further analysis. Data were analyzed with ACQUIS1 software (developed by G. Sadoc for the Centre National de la Recherche Scientifique). The bandpass of the recording system for field potentials was set at DC to 3 kHz, (for the WPI M-707A electrometer) or 0.1 Hz to 3 kHz (for the WPI DAM 80 differential amplifier).

A stereotaxic zero reference was defined for each experiment, usually as the most rostral bifurcation of the blood vessel that runs along the medial margin of the edge of the valvula fold. This point is generally ~1200 μm lateral to the midline and the same distance caudal to the front of the C1 lobe of the cerebellum. Electrodes were angled ~2° lateral to the vertical axis of the fish. Tracking was begun 400–500 μm medial and 300–500 μm rostral to the stereotaxic zero point. Physiological identification of the precommand nucleus from recorded field potentials is described in Results.

In some experiments, the single-barrel electrode was replaced with a triple-barrel electrode (diameter of the tip of each barrel, ~2 μm) once the location and depth of the PCN were ascertained. The three barrels contained, respectively, L-glutamate (Sigma; 0.1 M in water, pH 8.0), Neurobiotin (Vector Laboratories, Burlingame, CA; 2% in 1 M KCl) and 3 M NaCl. To label recording sites, Neurobiotin was ejected iontophoretically with pulsed positive current (10 sec on, 3 sec off; 2–5 μA for 30 min). In other experiments, smaller deposits of horseradish peroxidase (HRP; 5% in isotonic NaCl) were used to label precise sites where maximum amplitude field potentials were recorded (tip positive, 1 μA for 1 min.). Neurobiotin labeling was developed using the ABC technique (Vector), and HRP labeling was revealed using the Hanker–Yates procedure modified by Bell et al. (1981).

While tracking through the brain, electrical microstimulation was used to identify points from which the electromotor system could be driven with a low threshold. Constant current (1–10 μA) square pulses of 0.2 msec duration or longer lasting DC currents (1–5 μA), were delivered directly through the micropipette containing 3 M NaCl. L-Glutamate iontophoresis (negative currents of 0.1–2 μA), which selectively stimulates cell bodies and dendrites but not fibers of passage, was used to stimulate PCN neurons chemically and thus to explore the effect of PCN neuron activity on the electromotor activity of the fish.

Peripheral electrosensory stimuli were applied using a stainless steel dipole (6 cm between electrodes) placed parallel to the fish at a distance of 5 cm, with the negative pole toward the head (potential gradient close to fish skin: 10–100 mV/cm). Monophasic square stimulus pulses of 0.5 msec duration were triggered by the EMN volley with a delay of 100 msec. This type of stimulation is not identical to a natural EOD but is effective in eliciting EOD responses in the behavioral context (Serrier, 1982).

Histology. After each experiment, the fish was reanesthetized deeply with MS-222 (concentration, 1:15,000) and perfused via the heart with fixative containing 2.5% formaldehyde and 2.5% glutaraldehyde in 0.1 M phosphate buffer, pH 7.4. Electrode tracks and the site of HRP deposit were reconstructed in the light microscope, from 80-μm-thick cresyl violet or neutral red counterstained sections.

RESULTS

The PCN region (Fig. 1*A*) has not been explored electrophysiologically previously, and although it is known that PCN axons project to the electromotor CN, it was not certain that an endogenously active motor-related field potential would be recorded at this site. For this reason, in preliminary experiments, microstimulation (1–10 μA) was used to find sites in the deeper regions of the midbrain from which the electromotor pathway could be driven with a low threshold. It was then observed that small electromotor-related field potentials were recorded at points where the threshold

for electromotor activation was lowest. These sites were labeled by deposit of HRP or Neurobiotin. Histology showed that these recording sites corresponded to the anatomical description of PCN (Grant et al., 1999). The electromotor-related field potentials, unit activity, and electrosensory responses of PCN are described below.

Field potentials in PCN

The typical field potential recorded in the center of PCN is illustrated in Figure 1, *B* and *C* (*middle traces*); this was recorded at a depth ranging from 3550 to 5800 μm from the dorsal surface of the brain, depending on fish size and electrode angle. PCN could be reliably identified by a two-peaked negative field potential, followed by a slow positive potential that was always associated with every EMN volley. The three components of the PCN field potential varied in size in the different regions within the nucleus. The slow positive potential (Fig. 1*B, middle trace, arrow*) was largest in amplitude in the center of the nucleus. In the more caudal regions of PCN, from which descending axons exit in a medioventral direction, the first negative peak was large, and the second negative peak was less prominent; the slow positive potential was small. Toward the rostral pole of PCN, the initial negative peak and the slow positive potential were small or absent, and multiunit bursting activity of the sort illustrated in Figures 8 and 9 was predominant. Neurons in this region of the nucleus are smaller (K. Grant and G. von der Emde, unpublished observations), and it is possible that they form a functional population that is different from that formed by neurons in the center and caudal region.

The first negative peak of the PCN field potential preceded T_0 by a constant fixed interval (Fig. 1*B*). In most fish this interval was ~2.2 msec (Fig. 2*B,C*). The second negative peak of the PCN field potential varied more in amplitude and timing at any given site; in certain records it was barely visible. It occurred between 0.75 msec before and 0.55 msec after T_0 (Figs. 1*B,C,* 2*B,C*). The slow positive field potential followed the negative peaks, reaching a maximum after 8–12 msec and lasting for 20–40 msec (Figs. 1*B*, 2*A*). This positive wave was characteristic of PCN and was recorded only in the region containing PCN cell bodies; it could usually be detected on an audio-monitor before it became visible above the background noise level on the oscilloscope trace and it was of particular value in distinguishing the nucleus field potential from other EOD command-related events occurring in neighboring regions.

PCN axons project to the command nucleus in the medulla (Bell et al., 1983), and thus the field potentials were compared in the two nuclei. Recorded in the same fish, the first negative peak in CN preceded the first negative potential in PCN by 0.7 msec (Fig. 1*C*). This shows that the first negative peak of the field potential in PCN is a consequence and not a cause of activity in the command nucleus. The second negative peak in PCN was more variable in form and timing than that in CN, but when it did occur, it appeared later than the second negative peak in CN.

Because motor-related activity began later in PCN than in CN, it is possible that the field potentials recorded in PCN were the result of electromotor command corollary discharge activity. PCN field potentials were thus also compared with those recorded in the nearby MCA. MCA receives excitatory input via a disynaptic pathway from CN (Bell et al., 1983; Grant et al., 1986; Bell and von der Emde, 1995) and is the midbrain relay of the corollary discharge pathway. It is situated in approximately the same rostrocaudal plane as PCN, ~1 mm dorsal and 200 μm lateral, and was often recorded in the same electrode tracks as PCN.

The MCA field potential also had two prominent negative peaks (Fig. 2*A, bottom trace*), although its form was often more complex than that recorded in either PCN or CN (Aljure, 1964; Bell et al., 1995). Comparison showed that the first negative peak of the field potential in PCN always occurred earlier (~0.2 msec) than the earliest negative peak recorded in MCA (Fig. 2*B,C*). Similarly, the second negative peak in PCN almost always occurred earlier than the second negative peak of the MCA field potential, although in a few cases the timing was reversed (Fig. 2*C*). In general, the occurrence of the second negative peak in MCA was variable, and its

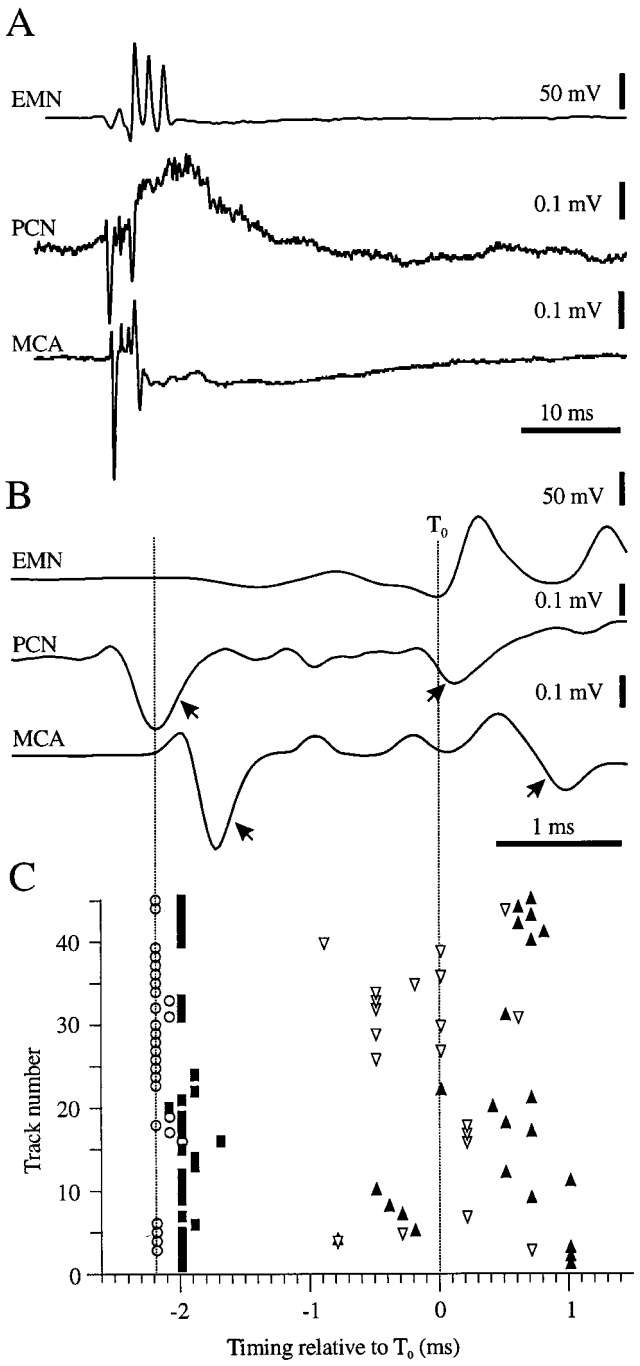

Figure 2. Comparison of the timing of electromotor-related activity in PCN with the corollary discharge-driven field potentials seen in MCA. Field potentials from the two nuclei were recorded successively in the same electrode track. *A*, *B, Top traces,* Electromotoneuron triple volley (average, $n = 39$); *bottom traces,* averaged traces of extracellular field potentials in PCN ($n = 15$) and the MCA ($n = 39$) recorded in the same fish. Note that electromotor field potentials begin earlier in PCN than in MCA—the most extreme example is illustrated. In PCN a characteristic slow positive wave follows the two initial negative peaks (*A, middle trace*), whereas in MCA, a slow negative wave occurs at this time (*A, bottom trace*). *C,* Comparison of the timing of negative peaks of the PCN and MCA field potentials (*B, arrows*) recorded successively in the same electrode tracks (data pooled from 11 fish). *Open symbols*, Negative peaks in PCN; *filled symbols,* negative peaks in MCA. The first electromotor-related events occurred 2–2.2 msec before T_0 in PCN and ~0.2 msec later in MCA. The relative timing of later negative peaks occurring in PCN and MCA was less constant.

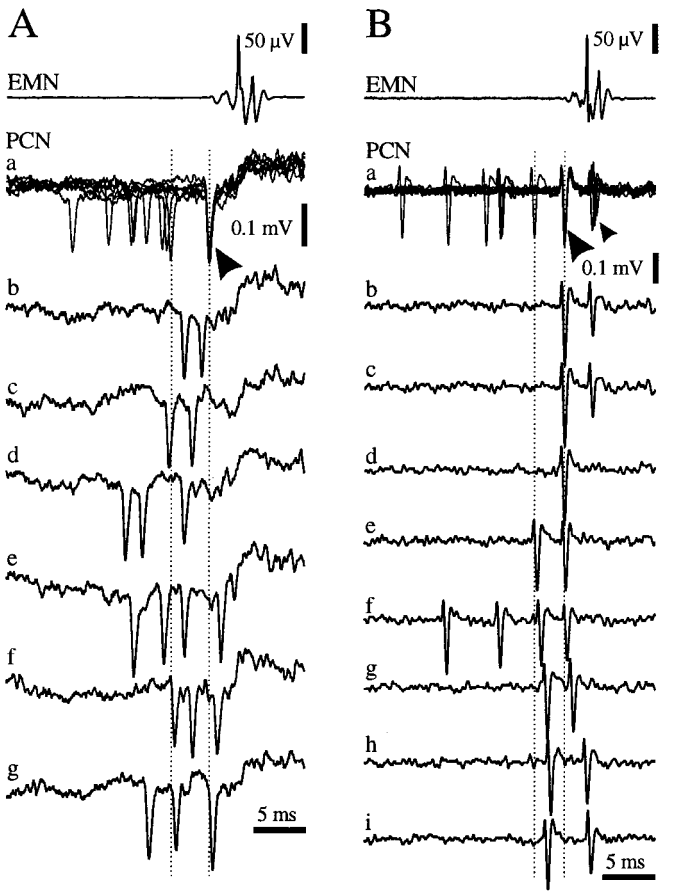

Figure 3. Spontaneous unitary spikes in PCN and occlusion of electromotor-related spikes. *A*, *B,* Two examples of units that fired spontaneously preceding electromotor activation. *Top traces,* Electromotoneuron triple volley. Traces in *A* are presented without filtering; traces in *B* were filtered to eliminate the slow positive wave that normally follows the negative motor-related events, to facilitate spike-timing analysis. In *Aa* and *Ba*, in the majority of cycles (selected superimposed traces), the timing of one unit spike had a fixed latency relative to T_0 (*large arrows*); the other spikes appear sporadically. In *B* (*Bb* and *Bc, individual traces*), a second motor-related spike frequently occurred a little later (*small arrow*), corresponding to the timing of the second negative peak of the PCN field potential, but its timing was less constant, and it was sometimes absent (*Bd–Bg*). In both *A* and *B*, when spontaneous unit spikes occurred within the period between the *vertical dotted lines*, the fixed latency motor-related spike was either absent (*Ac–Ad*, *Bh,i*) or delayed (*Ae–Ag, Be–Bg*). For explanation of apparent occlusion, see Results.

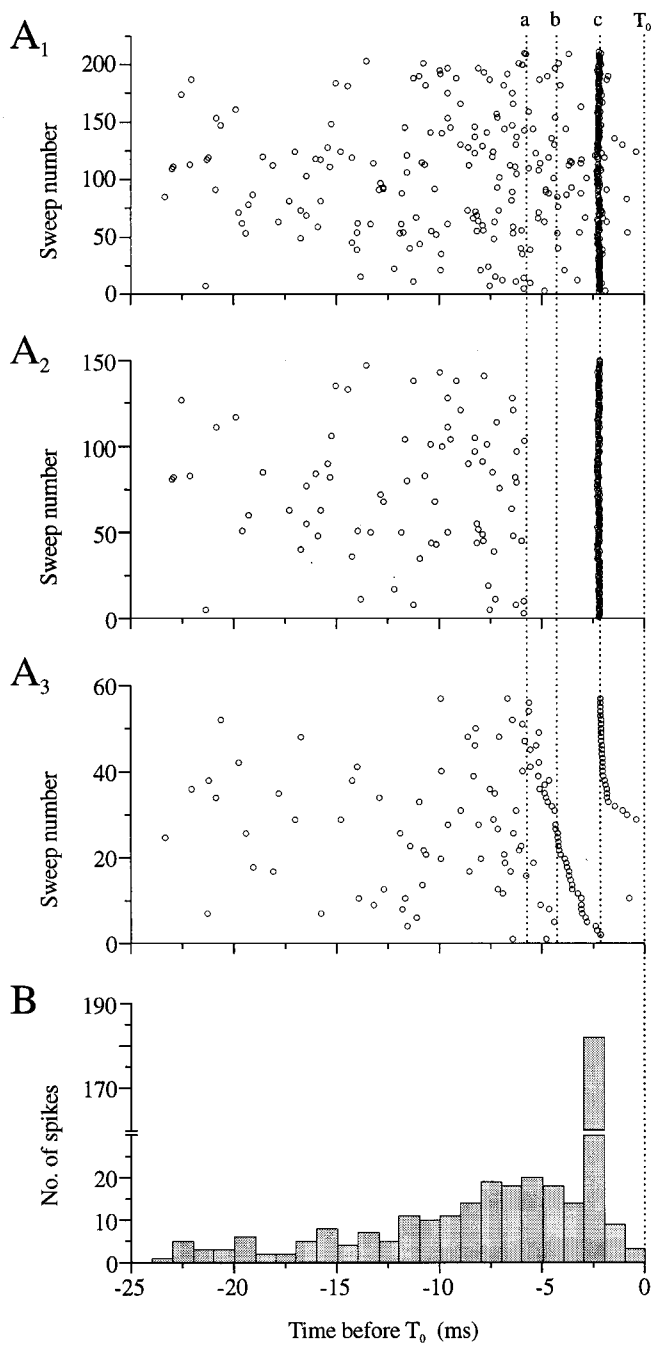

Figure 4. Occlusion of motor-related unitary firing (data from unit in Fig. 3*A*). A_1–A_3, Precommand raster diagrams show timing of spikes relative to T_0. A new sweep was triggered by each EMN volley. A_1, Spike firing during successive inter-EMN cycles, presented in the natural order of occurrence. A_2, A_3, Cycles have been reordered to illustrate occlusion period of fixed-timing motor-related spike. A_2, Cycles in which a fixed latency motor-related negative spike occurred within ±0.08 msec of the mode of the spike timing histogram shown in *B* (2.2 ± 0.08 msec before T_0). *A3,* Cycles in which the motor-related first negative spike was either delayed (sweeps 29–60) or absent (sweeps 1–28). *Vertical dotted lines* indicate the mean latency (2.2 msec) of the fixed motor-related negative spike (Fig. 3*A, large arrow*) (*c*); a period during which, if a spontaneous spike occurred, the motor-related spike was delayed (*a,b*); and a period during which if a spontaneous spike occurred, the motor-related spike was absent (*b,c*). Points *a* and *b* are 5.8 and 4.3 msec, respectively, before T_0. *B*, Histogram showing cumulated spike firing pattern for period 25 msec before T_0.

timing was not strictly correlated with that of the second negative peak in PCN. Thus, the second negative peaks of the PCN and MCA field potentials were probably neither causally related nor of common origin. The latencies of the negative field potentials recorded in PCN and MCA are compared in Figure 2*C*. It is also interesting to note that in MCA, the two initial sharp negative peaks were followed by a slow negative field potential lasting up to 30 msec (Fig. 2*A, bottom trace*), in contrast to the slow positive potential observed in PCN (Fig. 2*A, middle trace*).

Unitary activity in PCN

Two different sorts of unitary action potential activity were recorded extracellularly in PCN: (1) tonically active units that fired spontaneously with an irregular rhythm, some increasing their frequency just before the initiation of the EMN volley, but that were always silent for 20–70 msec immediately after the EMN volley (Figs. 3–6), and (2) units that fired a burst of action potentials during the period immediately after initiation of the EMN volley but that were otherwise silent (Figs. 7-9).

Many units of the tonically active first type fired mainly before initiation of the electromotor command and only sporadically at other times (Fig. 3). Other units of this type fired more continuously (Fig. 5), pausing only at the time of the EMN volley and for a short period afterward (Fig. 5*B*). Figure 3 shows that these units often fired an action potential at a fixed time before T_0 (Fig. 3*A,B,*

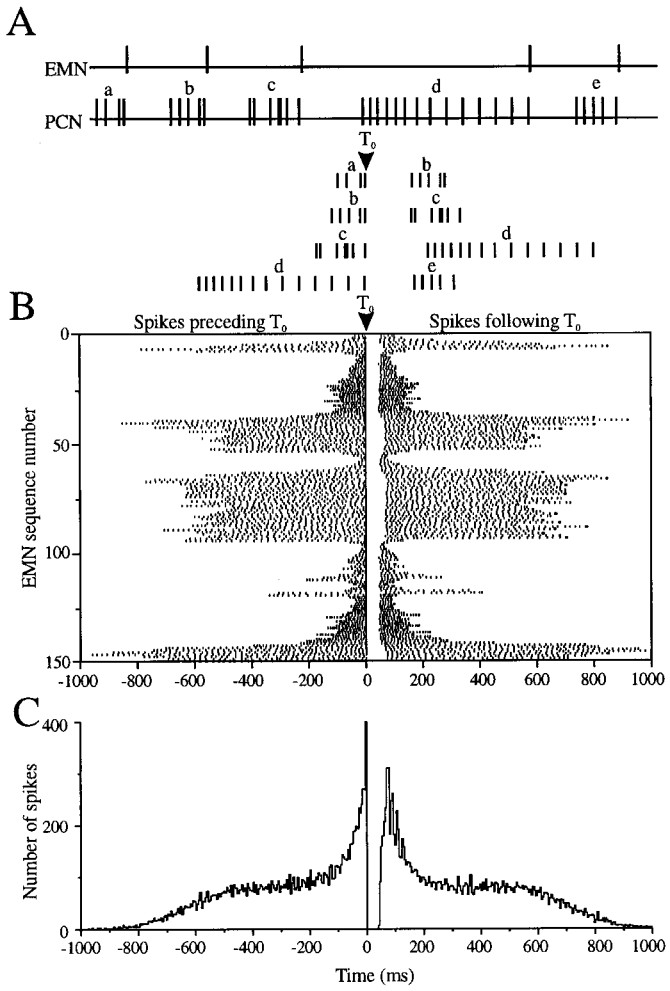

Figure 5. Example of timing of unit activity, firing tonically except immediately after the EMN volley. *A*, Method of construction of the raster shown in *B. Top trace* (EMN), Occurrence of EMN triple volley (T_0). *Bottom trace* (PCN), Spiking activity of PCN unit. Note that spike firing is always interrupted for several tens of milliseconds after the EMN volley. Letters *a–e* represent the successive episodes of spikes fired by the PCN unit between EMN volleys. Bursts *b–d* are each plotted twice: first after the current EMN volley and then again on the next line, before the next successive EMN volley. *B,* Peri-T_0 raster diagram showing spontaneous firing before and after EMN volley in successive cycles. Note that the right-hand envelope of the raster (from T_0 to the last spike in the line) can be interpreted as a plot of successive EMN intervals. *C,* Cumulated histogram of spike firing over 750 cycles. Note the silent period of ~50 msec always present after T_0.

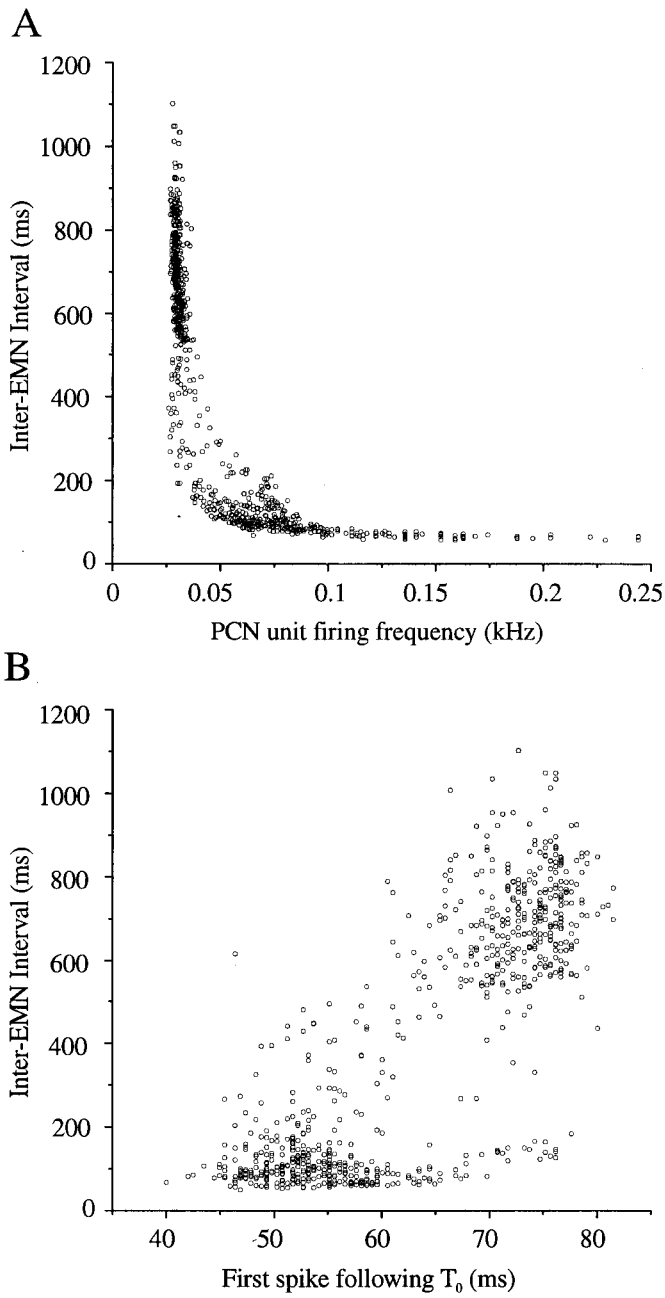

Figure 6. The relationship of spontaneous firing to the inter-EMN interval duration (same unit as in Fig. 5). *A,* Inter-EMN interval duration is plotted against mean firing frequency of the PCN unit, calculated over the period after the previous post-EMN volley silent period, until the current T_0. Transition from the basal mean firing frequency of ~0.03 kHz, to higher firing frequencies (up to 0.1 kHz), is inversely related to the duration of the inter-EMN intervals. *B,* Inter-EMN interval duration is plotted against the timing of the first spike after the post-EMN silent period. Inter-EMN volley intervals tend to be shorter when the first post-EMN volley spike occurs earlier.

superimposed traces), resembling the first negative peak of the motor-related field potential recorded at the same site (Fig. 1*C*). This suggests that the first negative peak of the PCN field potential is probably in fact a focal potential corresponding to the synchronous activation of a small number of units close to the electrode tip. However, when a unit potential fired within a time window of a few milliseconds immediately before the expected occurrence of the motor-related spike, the latter was either absent (Fig. 3*A, traces b–d*) or appeared to be delayed (Fig. 3*A, traces e–g; B, traces d–h*).

This phenomenon is illustrated over 200 electromotor command cycles in Figure 4 (the same unit as Fig. 3*A*). The upper raster (Fig. $4A_1$) shows the timing of unit spikes relative to T_0 for successive electromotor command cycles illustrated in the natural order in which they occurred. In some cycles the fixed motor-related spike was present, and in others it failed or was delayed. In the rasters of Figure 4, A_2 and A_3, the individual sweeps have been reordered to explore this further. Figure $4A_2$ shows those cycles in which a unit spike occurred exactly at the time of first negative peak of the field potential (at 2.2 ± 0.08 msec before T_0). Figure $4A_3$ shows spike timing in cycles in which the fixed-latency first negative peak was either delayed (sweep numbers 29–60) or did not occur (sweep numbers 0–28). Thus, the fixed timing motor-related spike only occurred if no other unit potential fired during a time window of 3.6 msec preceding the expected motor-related spike (period *a-c* in Fig. $4A_2$, i.e., 5.8–2.2 msec before T_0). The motor-related unit spike was present but delayed if other unit spikes fell within the period *a–b*, (Fig. $4A_3$) i.e., 5.8–4.3 msec before T_0, or 3.6 to 2.1 msec preceding the expected motor-related spike, and no motor-related spike occurred if other spikes fell within the period <2.1 msec preceding the expected motor-related spike (period *b–c* in Fig.

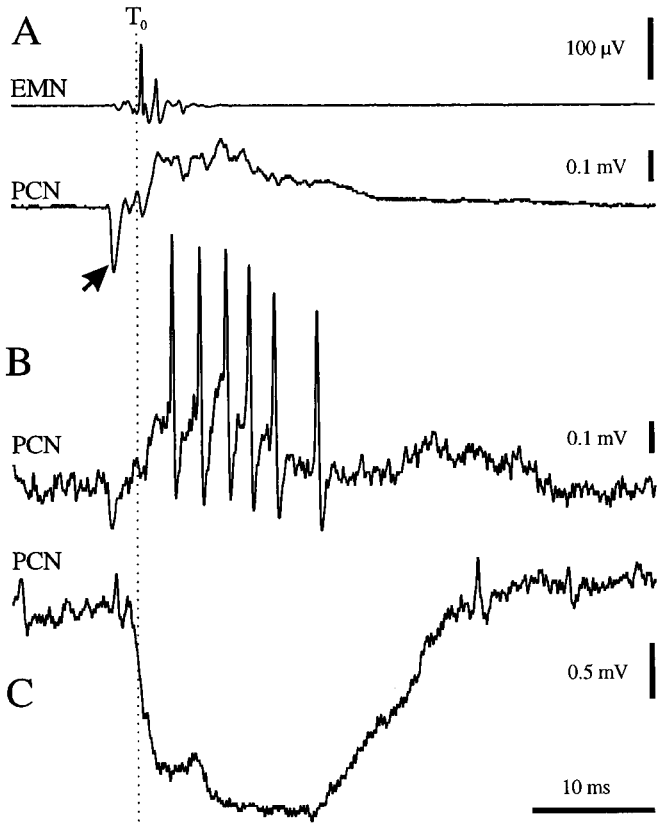

Figure 7. Unit activity during the slow positive PCN field potential. *A,* EMN triple volley and averaged extracellular field potential recorded in PCN ($n = 15$). *Arrow* indicates first negative electromotor-related negative peak of PCN field potential. *B,* Burst-type unit activity that occurs only during the period of the corollary discharge-related positive field potential. *C,* An intracellular record made at a distance of 100 μm from the unit in *B*, showing a large IPSP whose timing corresponds with that of the slow positive field potential and the burst activity recorded extracellularly.

$4A_3$, i.e., 4.3–2.2 msec before T_0). The distribution of all spikes firing before T_0 is shown in the histogram of Figure 4*B*.

This failure of firing resembles collision rather than refractoriness, because interspike intervals of <2 msec were observed in the spontaneous firing of this unit (e.g., Fig. 3*Aa*). It suggests that the fixed-timing motor-related unit spike may not have the same origin as the irregularly timed preceding spikes. The fixed-timing motor-related spike occurs ~0.7 msec later than activity in the command nucleus (Fig. 1*C*), but this interval is probably not long enough to include trans-synaptic feedback from the command nucleus via the known corollary discharge pathway. We therefore suggest that the fixed-timing PCN spike may result from antidromic invasion of PCN axons terminating on CN neurons, at the moment of the synchronous firing of CN neurons that drives the descending electromotor pathway. This antidromic backpropagation may be initiated across electric synapses because the ultrastructural study by Elekes and Szabo (1985) showed that the majority of synapses contacting CN neuron somata contain gap junctions (see Discussion).

The period in which spiking was not followed by a motor-related spike is close to the occlusion period that would be expected if the motor-related spike in the PCN unit were driven by antidromic invasion from the postsynaptic command neurons, which can be calculated as the sum of the conduction time from PCN to CN, plus the refractory period of the PCN axon, plus the conduction time from CN to PCN, i.e., 0.7 + (~ 1) + 0.7 = 2.4 msec. (The conduction time from PCN to CN was calculated as 0.7 msec, taken as the difference between the first negative peaks of the field potentials in PCN and CN illustrated in Fig. 1*C*.)

The unit in Figure 3*B* shows records from another site, illustrating a second, later motor-related unit potential that corresponded to the timing of the second negative peak of the PCN field potential observed in other recordings (Figs. 1*B,C,* 2*A,B*). The timing of this second motor-related spike was variable, and it was not always present.

Figure 5 illustrates the tonic firing pattern of a similar unit that was continuously active, except immediately after initiation of the EMN volley. To understand how spontaneous unit firing in PCN might be related to the length of inter-EMN intervals, a peri-EMN raster diagram was constructed showing all spikes occurring before and after T_0, over 150 EOD command cycles. The method of construction is described in Figure 5*A*. In each line of the raster, all spikes occurring before each EMN volley were plotted to the left of T_0; the length of the silent period and all spikes occurring after each EMN volley (and before the next EMN volley) were plotted to the right of T_0. The succeeding lines in the raster thus describe the unit firing before and after successive motor commands. The symmetry of the plot arises because each PCN spike is represented twice in the raster: once to the left of T_0 (if it occurred in the interval preceding the current EMN volley) and once to the right of T_0 (if it occurred in the interval after the current EMN volley). In this graphic representation, the right-hand envelope of the raster may be interpreted as a sequential plot of the EMN intervals.

For the unit activity illustrated, tonic firing frequency and the length of the silent period after the EMN volley were both related to the length of the inter-EMN interval (Fig. 6). When PCN unit firing frequency was high, inter-EMN intervals tended to be short, and vice versa (Fig. 5*B*). This behavior is quantified in Figure 6*A,* which shows a negative correlation between inter-EMN interval length and PCN unit firing frequency. When the electromotor command cycle length was >500 msec, a basal unit firing frequency (0.03 kHz) appeared to have been reached.

The length of the inter-EMN interval was also correlated with the latency of the first spike after T_0 and thus with the duration of the post-EMN volley pause (Fig. 5*B*). However, the distribution of points in Figure 6*B*, showing the timing of the first PCN spike after the EMN volley, suggests that there are two preferred pause lengths (~45–60 and 65–75 msec), or two preferred inter-EMN intervals, rather than a continuous interdependent variation. Similar bimodal interval distributions are frequently observed in the naturally occurring electromotor rhythms (Teyssedre et al., 1987).

The second type of unit recorded in PCN fired a burst of action potentials during the slow positive wave of the PCN field potential (Fig. 7*A,B*). At all other times such units were silent. Here we associate the observation that in five short intracellular recordings made in the PCN, a large, two-component IPSP was present, which also coincided with the slow positive potential seen extracellularly (Fig. 7*C*). It seems probable that this IPSP, which inverted with intracellular injection of chloride ions, is related to the action potential burst seen in the type 2 bursting units described here. Together these events may reflect a corollary discharge-driven inhibitory input to PCN.

In most units of this second type, the structure and timing of the burst of action potentials was rather constant, although from one unit to another the exact timing of the first spike of the burst and number of spikes per burst differed (compare the three examples in Fig. 8*A*). For any given unit, the timing of the first spike in each burst was remarkably constant. Later spikes showed more variability, and the last two or three spikes of longer bursts were not always present (Fig. $8A_{1-3}$, *histograms*) thus producing bursts of varying duration. The units illustrated in Figure 8 were recorded during EOD command firing at a relatively low endogenous rate (Fig. 8*B*), and under these conditions no correlation was found between inter-EMN interval and first spike timing (Fig. 8*C*) or between inter-EMN interval and burst duration (Fig. 8*D*).

For a fourth unit of this type, however, a relationship was found between burst timing, burst structure, and inter-EMN interval (Fig. $9C_{a-c}$). Figure 9*A* shows that the timing of the spikes within this burst was less precisely fixed than for the units illustrated in Figure 8. In addition, the distribution of inter-EMN intervals for the

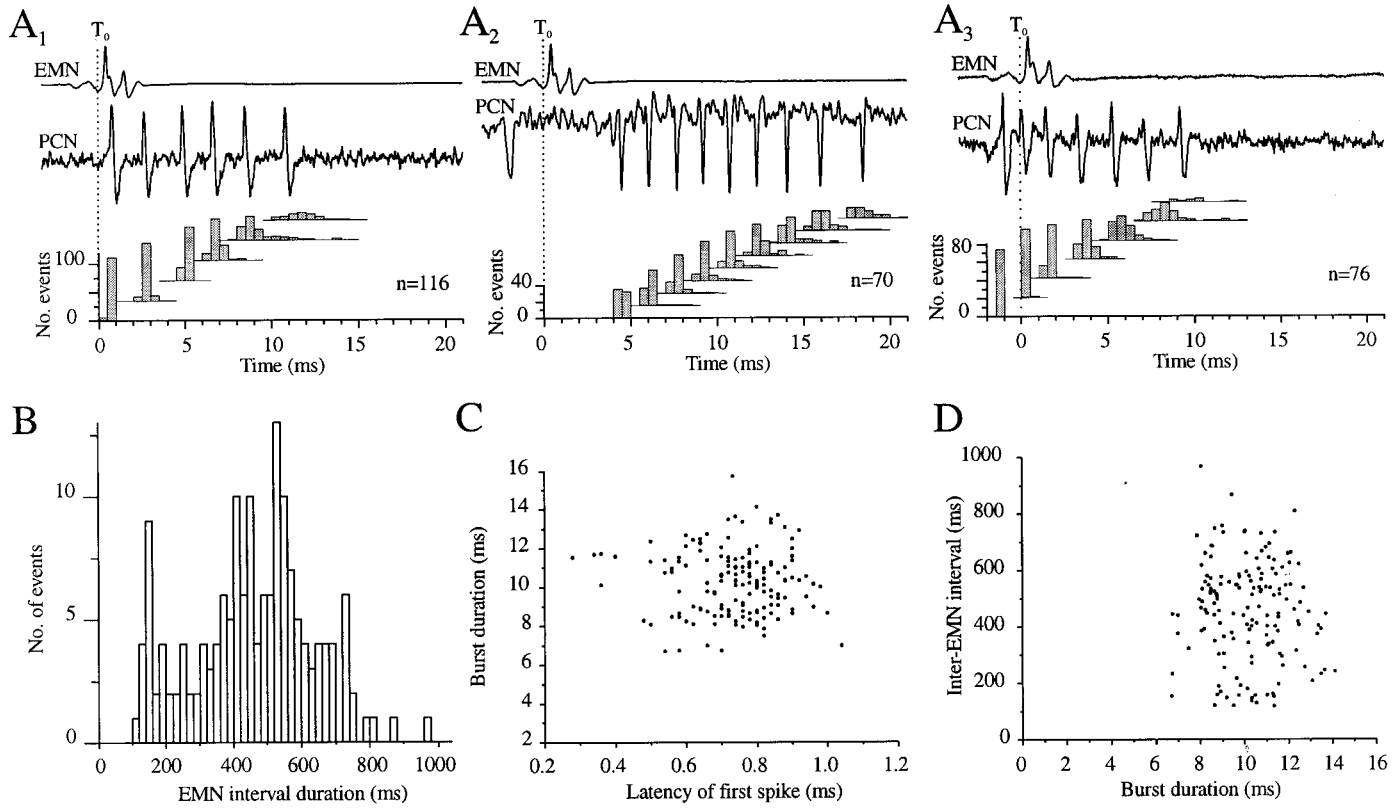

Figure 8. Post-EMN volley bursting units fire stereotyped sequences of spikes with individually different timing. *A,* Three different units recorded in PCN that fired a burst of action potentials during the time of the slow positive field potential (see Fig. 7), each with a different timing relative to T_0 (AC-coupled records that filter slow positive field potential). The timing of action potentials in the individual bursts was extremely constant—see histograms constructed over *n* cycles, below each set of traces. *B–D,* Data for the first unit illustrated in *A. B,* Histogram of inter-EMN intervals constructed over 86 cycles (peak between 400 and 600 msec). *C, D,* Plots of burst duration against latency of the first spike of the burst occurring after T_0 (*C*), and of inter-EMN interval against burst duration (*D*) show that there was no significant correlation between these parameters (df = 115; $r = -0.14$; $p > 0.05$ for *C*; $r = -0.17$; $p > 0.05$ for *D*) (the same analyses performed for the second and third units in *A* gave similar results).

period during which this record was obtained (Fig. 9*B*) shows that the endogenous rhythm of the electromotor command was faster than that illustrated in Figure 8*B* and that most inter-EMN intervals fell between 100 and 200 msec. In this case, the latency of the first spike of the burst was negatively correlated with the inter-EMN interval: when the first spike occurred earlier, the following inter-EMN interval was longer (Fig. 9*Ca*). This negative correlation was more highly significant for data from electromotor command cycles in which the inter-EMN interval was <200 msec: the regression line for these points is drawn in Figure 9*Ca*. Inter-EMN interval was less closely related to first spike timing when electromotor command cycles were >200 msec. Inter-EMN interval was also correlated with burst duration and intraburst frequency (Fig. 9*Cb,Cc*), and this correlation was again only significant for data obtained from cycles in which the inter-EMN interval was <200 msec.

PCN responses to electrosensory stimulation

An electrosensory stimulus played to the fish through electrodes placed in the water evoked an electromotor response with an EMN volley (T_0) latency of 14–15 msec. In PCN, the field potential that accompanied this evoked electromotor activity was identical to that which occurred in association with intrinsic spontaneous activation of the motor command (Fig. 10, compare *A, B*). However, the electrosensory stimulation evoked specific, additional unitary activity that preceded the first negative peak of the PCN field potential (Fig. 10*B, small arrow*). A single electrosensory stimulus at twice threshold strength evoked one to three spikes with a variable latency between 8 and 14 msec (Fig. 10*B,C*). With repetition of the sensory stimulus, the latency of the evoked electromotor response increased (Fig. 10*D*), and after 8–10 trials the motor response occasionally even failed, although the sensory evoked unit activity in PCN was nevertheless still present (Fig. 10*C*). This suggests that adaptation, or an increase in threshold for the motor response, occurs at some other site.

Electromotor behavior evoked by stimulation in PCN

Electromotor activity could be evoked at short latency (~4–8 msec) by microstimulation in PCN. For brief depolarizing DC pulse stimuli (0.1 msec) given via the recording microelectrode, thresholds ranged from 0.4 to 1 μA in the center of the nucleus. However both threshold and latency of the motor response depended on the time elapsed between the stimulation pulse and the preceding EMN volley.

In the center of the nucleus an electromotor response to microstimulation at twice threshold intensity was obtained with a latency of 4–5 msec, provided that the delay between the preceding EMN volley and the stimulus was >50 msec (Fig. 11*A*, *top trace*, *B*). At shorter EMN-stimulus intervals this short latency motor response generally failed (Fig. 11*A*, *bottom trace*, *B*), although in some cases, depending on the stimulation site, increasing stimulus strength could reduce the apparent "refractoriness" to 20–40 msec. When stimulating in the center of PCN, no short latency response could be evoked at EMN stimulus intervals <20 msec.

Refractory periods to stimulation in PCN were shorter in the caudal region of the nucleus, possibly because here some of the efferent axons projecting to CN were being stimulated directly and the effects of corollary discharge feedback inhibition (see below) were less strong. In the example illustrated in Figure 11*E–H*, as the interval between the preceding EMN volley and the stimulus was deceased, a step change in the evoked EMN response latency, from ~5 msec to a more variable value between 20 and 25 msec was

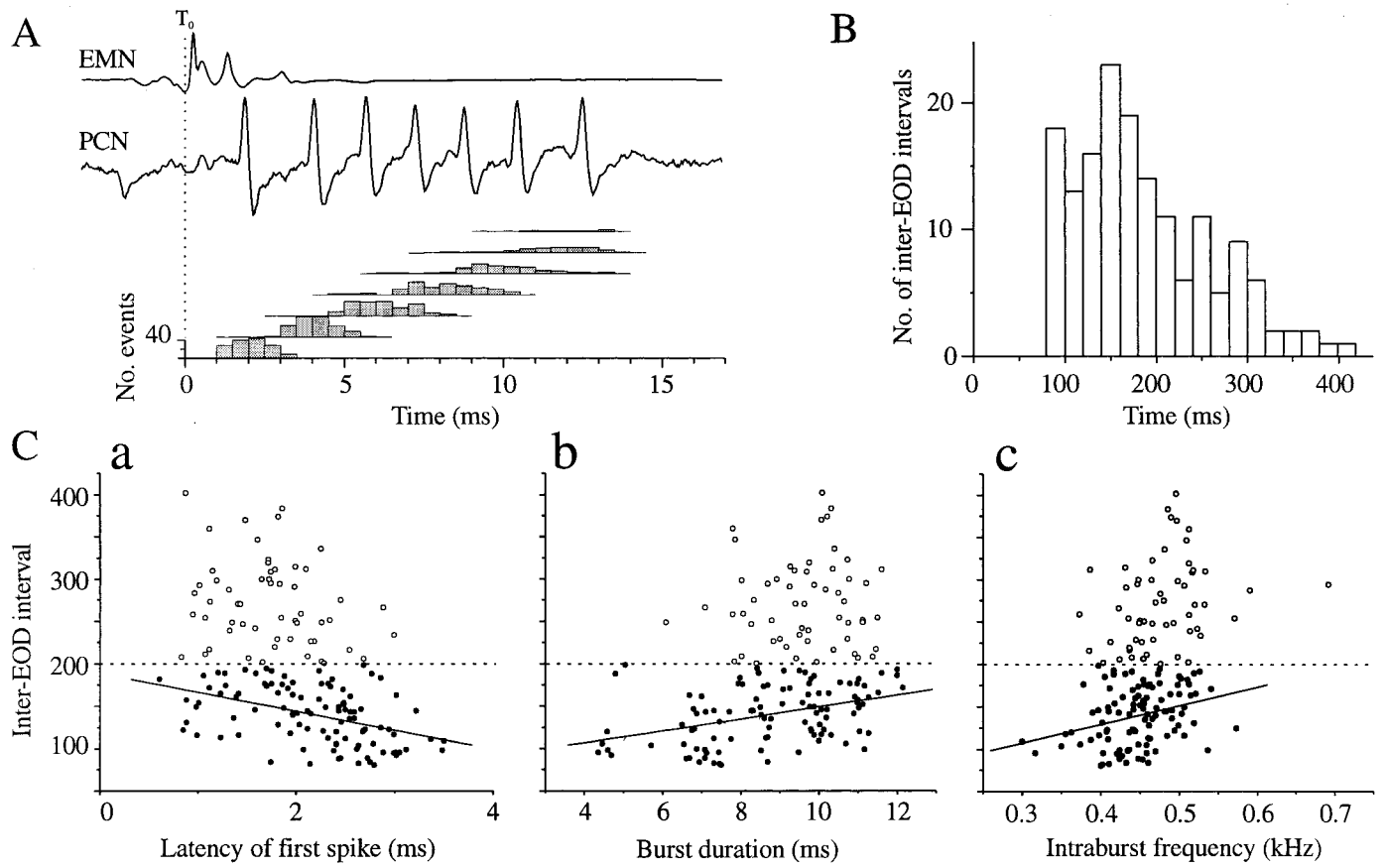

Figure 9. The post-EMN volley burst activity is correlated with inter-EMN volley interval when the intrinsic EOD command rhythm is rapid. *A,* EMN volley, extracellularly recorded burst activity, and spike latency histogram for a fourth unit recorded in PCN (AC-coupled record), during relatively rapid firing of the intrinsic electromotor command. The timing of spikes within the burst was less constant for this unit than for the units illustrated in Figure 8. *B,* Histogram of inter-EMN intervals over the recording period, showing that the intrinsic rhythm of the EOD command center was faster during this recording (peak at 150 msec) than during those shown in Figure 8. *C,* Plots show an inverse correlation between inter-EOD interval and latency of first spike in burst (*Ca*), and direct correlation between inter-EOD interval and burst duration (*Cb*), and inter-EOD interval and intraburst firing frequency (*Cc*). These correlations are only significant for points obtained when the EMN interval was ≤200 msec (df = 102; $r = -0.44$; $p < 0.001$ for *Ca*; $r = 0.4$; $p < 0.001$ for *Cb*; $r = 0.3$; $p < 0.002$ for *Cc*). Regression lines are shown in each plot for points in which inter-EMN interval was <200 msec.

frequently observed (Fig. 11*E,* compare *top* and *middle traces*; see plots in Fig. 11*F,G*). This bimodal distribution of the evoked motor response latency (Fig. 11*G*, *black bars*) produced a discharge pattern similar to the alternating short intervals of rapid electromotor behavior observed during active electrolocation and in social encounters (Moller, 1970; Bell et al., 1974; Moller et al., 1989).

Microstimulation in PCN also induced a regularization of the spontaneous motor command rhythm. After a directly evoked short latency motor response, there was a considerably higher than normal probability that the next, subsequent EMN volley would occur after an interval of 100 msec (Fig. 11*B,C, h, E,F, h′*). In addition, when the short latency evoked response failed because of refractoriness, the first subsequent EMN volley occurred with a rather constant latency of 70–80 msec (Fig. 11*B,F,G*). The spontaneous intrinsic motor command rhythm then returned to the usual irregular pattern and in both cases, the next subsequent inter-EMN interval followed the same pattern of variability as the normal spontaneous interval distribution (Fig. 11*D,H*). The phenomenon underlying this regularization thus lasted for 100–200 msec, although its precise mechanism is not yet known.

Stimulation in caudoventral sites, probably within the descending axon tract leaving PCN in the direction of CN, could drive the electromotor pathway at much higher rates, down to inter-EMN intervals of as little as 4–5 msec. During such rapid repetitive activation of the electromotor pathway, the rate-limiting factor appeared to be the integrity of the triple action potential volley fired by the electromotoneurons (Aljure, 1964; Bennett et al., 1967). At high firing rates, the third action potential of the EMN volley tended to drop out, and if the stimulus was repeated as a train, the EMN volley became unsynchronized and disorganized.

In addition to brief electrical stimuli, we also used longer lasting DC electrical stimuli to drive the electromotor system from within PCN. Figure 12*A* shows that electrode tip-positive stimulation with an intensity of 1.5 μA caused a threefold tonic increase in EMN firing frequency. The absolute magnitude of the increase in firing rate depended on stimulus intensity. In contrast, tip-negative stimulation caused marked transient increases in discharge rate at the onset and termination of the stimulus pulse, but no tonic frequency increase during the DC stimulus plateau (Fig. 12*B*).

Iontophoresis of L-Glutamate in PCN also caused a tonic increase in EMN firing rate whose pattern resembled that evoked by DC electrical stimulation. This effect was dose-dependent, and spontaneous additional increases in firing rate could be superimposed on the drug-induced response (Fig. 12*C*). The lack of any response to reversed polarity iontophoresis in the control trace of Figure 12*D* shows that the observed effect was caused by L-Glutamate and not by current injection.

DISCUSSION

Our results confirm that in the mormyrid *Gnathonemus petersii,* the bilateral midbrain precommand nucleus modulates the activity of the electromotor command center and mediates both sensory-based behavioral responses to environmental stimuli and endogenously initiated social display patterns. We suggest that by its position and functional role in the electromotor system, it is func-

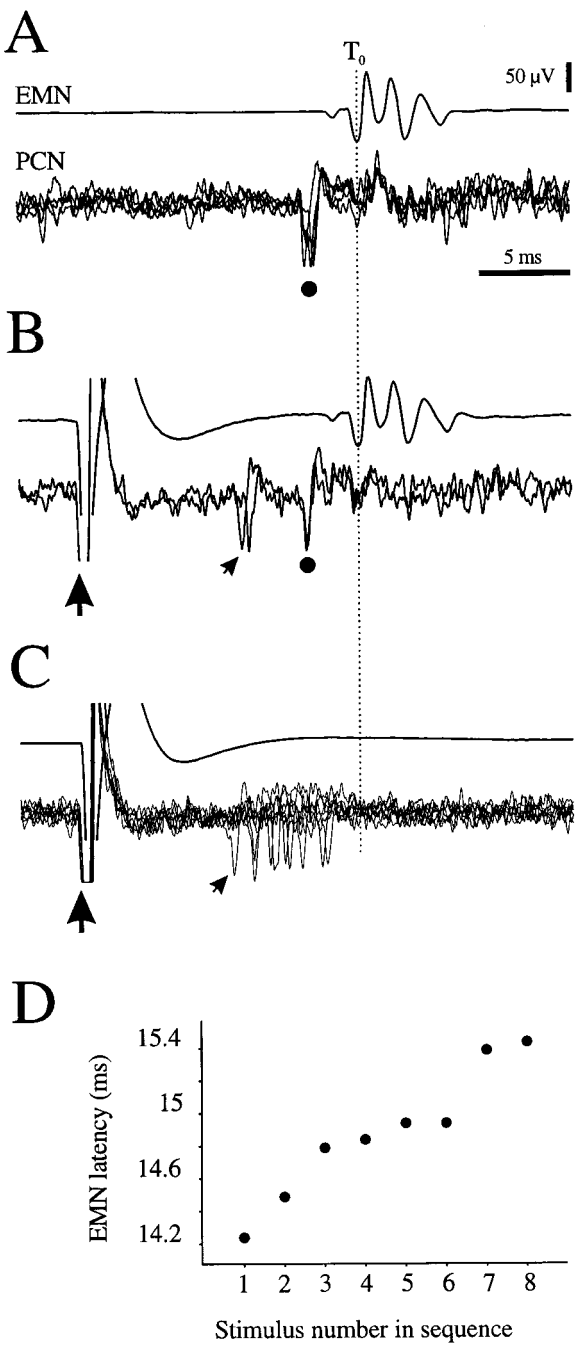

Figure 10. Electrosensory-evoked unit activity in PCN. *A, Top trace,* Spontaneous electromotoneuron volley (average of 4 traces); *bottom traces,* AC-coupled record of electromotor-related field potentials (superimposed traces) recorded in PCN (●) during intrinsic spontaneous command of the electromotor rhythm. *B,* Electromotoneuron volley (*top trace*, average of 2 traces) evoked by electrosensory stimulation (*large arrow*), which is accompanied (superimposed *bottom traces*) by a fixed latency motor-related field potential (●) in PCN identical to that in *A*, and by preceding unitary activity with more variable timing (*small arrow*). *C,* After several cycles of electrosensory stimulation, the electromotor response adapted and did not always occur. However, selected traces ($n = 8$) show that the same electrosensory stimulus continued to evoke unit activity in PCN even though the EMN volley was absent. *D,* Plot showing that the latency of the EMN volley evoked by successive electrosensory stimuli increased with successive stimuli. Stimuli were delivered at intervals of ~1 sec, triggered by a spontaneous EMN volley with a delay of 100 msec.

tionally equivalent to midbrain premotor areas that have been shown to modulate the activity of central pattern generators controlling skeletal motricity and a variety of stereotyped motor behaviors, in many vertebrates (Grillner et al., 1995).

The origin of field potentials in PCN

Motor-related field potentials in PCN were linked in a one-to-one manner, and with a fixed time relationship, to the command of the electric organ discharge but occurred later than the two-peaked negative field potential recorded in CN. Because no large precommand field potential was recorded in PCN preceding activation of the CN, it is concluded that PCN neurons do not fire in synchrony before initiation of the EOD command and that the electromotor related field potentials recorded in PCN do not represent events driving the electromotor command. We suggest instead that they reflect backpropagation of motor command activity or that they are evoked by ascending corollary discharge activity (Bell et al., 1983, 1995).

The first and second negative peaks and the following slow depolarization recorded in PCN probably have a different origin. It is possible that the first negative peak, which occurs ~2.2 msec before the EMN volley could be evoked via a collateral branch of the corollary discharge pathway (Fig. 13*A*). BCA axons projecting to MCA almost certainly run through the dendritic field of PCN neurons (Niso et al., 1989) and could have been recorded in the present study, although no BCA axon terminal field has yet been described in the region of PCN (Bell et al., 1983). However, the short delay between the first negative peaks of the field potentials in CN and PCN (0.7 msec), the lack of intrinsic sporadic firing in BCA axons (Clausse, 1985), and the apparent collision illustrated in Figures 3 and 4 make the validity of this hypothesis unlikely. An input from CN, via BCA and MCA to PCN can be excluded, because the onset of field potentials in PCN occurs earlier than those in MCA.

An alternative explanation is that the first negative peak recorded in PCN is the result of backpropagation of action potentials in PCN axons terminating on CN neurons that occurs at the moment when synchronous firing of the whole CN neuron population generates the descending electromotor command signal (Fig. 13*B*). This hypothesis is supported by the occlusion of the fixed latency unitary potential coincident with the first negative peak of the PCN field potential, observed when spontaneous unitary spikes occur in the preceding 2–3 msec. Occlusion could be caused by collision of an orthodromic action potential descending from PCN toward CN, with an ascending, antidromic action potential evoked in the PCN axon on firing of the postsynaptic CN neuron. This reasoning is supported by the observations of Elekes and Szabo (1985), who showed that the majority of synapses contacting command neuron somata form club endings containing gap junctions. Although these authors did not use specific labeling to identify their material, PCN axons constitute the major afferent pathway to the command nucleus (Grant and von der Emde, unpublished observation) and thus it is likely that their synaptic terminals are included in this population and that there may be electric synaptic transmission between PCN axons and CN neurons. The presence of gap junctions between PCN axons and CN neurons is also suggested by dye-coupled labeling of CN neurons observed after Neurobiotin deposit in PCN (von der Emde, unpublished results).

Other explanations for the generation of the first negative peak in PCN would require a hitherto unknown anatomical connection. It should be noted that no direct anatomical projection has been described from CN to PCN (Bell et al., 1983; Grant et al., 1986) and that insufficient time would be available for trisynaptic or multisynaptic projections from CN to PCN.

The origin of the second negative peak of the PCN field potential is less clear. It cannot be a correlate of the second negative peak of the CN field potential, which corresponds to the second action potential fired by command neurons and always occurs at a fixed latency relative to the EMN volley (Grant et al., 1986). The second PCN negative peak has a variable latency and is sometimes even absent. It seems probable that this event reflects input from the corollary discharge pathway, but as yet no possible anatomical pathway has been demonstrated.

The slow positive component of the PCN field potential occurred with a fixed timing relative to the motor command signal (EMN)

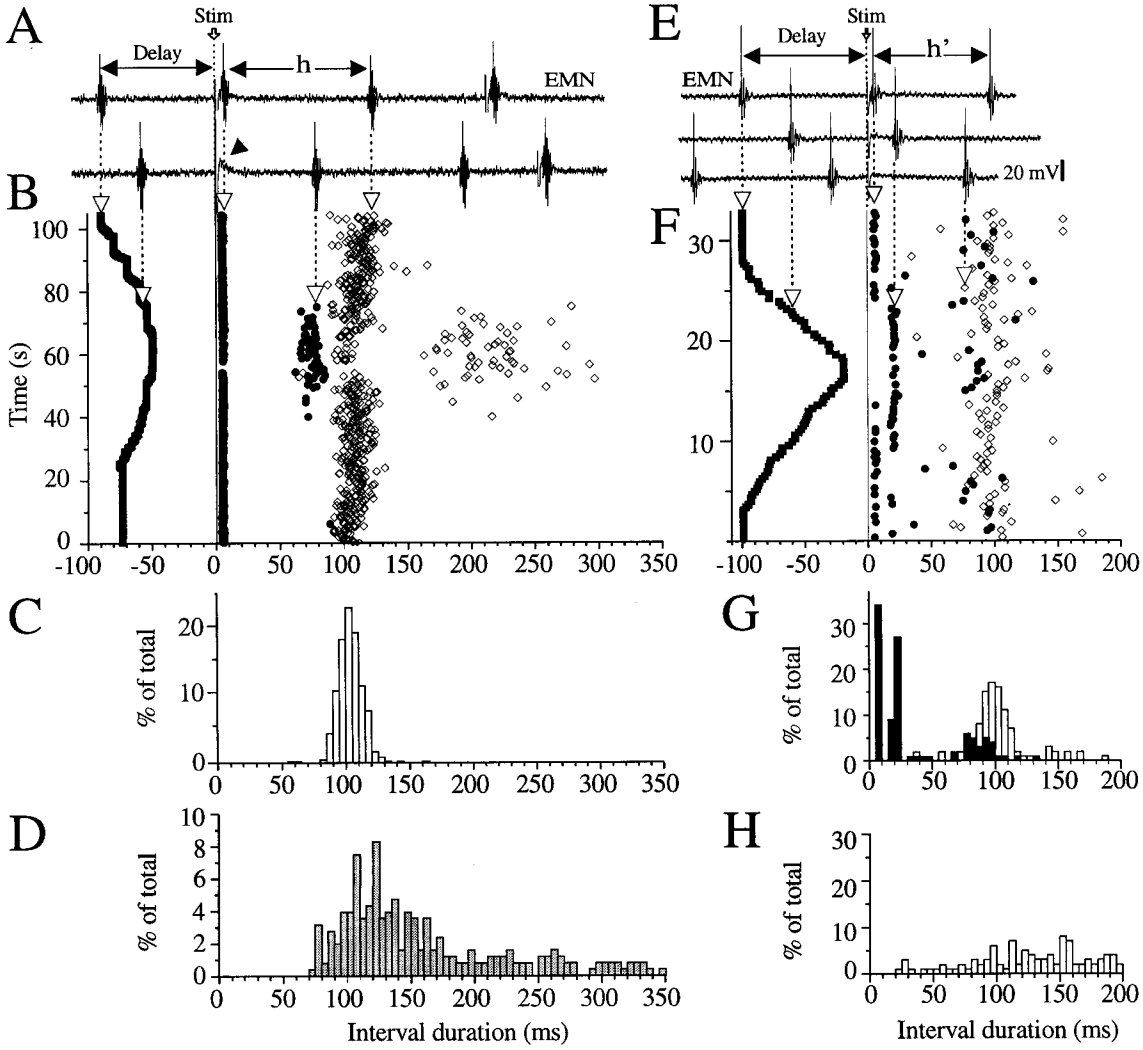

Figure 11. The electromotor pathway can be driven by electrical microstimulation in PCN. *A–D,* Responses to stimulation in the center of PCN. *E–H,* Responses to microstimulation in the caudal region of PCN. *A, E,* Records of EMN volleys. A single stimulus pulse (0.1 msec, twice threshold to evoke a response; *A, E, open arrow*) was delivered through the recording electrode in PCN, triggered at different delays after the EMN volley. The stimulus is represented at time 0 in the peristimulus raster diagrams in *B* and *F*. The timing of the preceding EMN volleys, used to trigger the stimulus is shown to the left of zero in *B* and *F* with a *filled square*. In *B* and *F*, the first EMN response after the stimulus is shown with a *filled circle,* and the second response after the stimulus is shown with an *open diamond*. *D*, *H,* The distribution of spontaneous inter-EMN intervals during this recording period. *A–D,* When the delay between the EMN volley and the stimulus was >60 msec (*A, top trace*), a short latency (~5 msec) electromotor response was evoked. The short latency response frequently failed when the EMN trigger-stimulus delay was <60 msec (*A*, *bottom trace, arrow*). However, in the case of failure, the next EMN volley always occurred in the period 50–80 msec after the stimulus. In stimulus cycles in which a short latency EMN response did occur, the next succeeding EMN volley also occurred at a rather fixed delay between 80 and 120 msec (*C, histogram*). In stimulus cycles in which the short latency response failed and the first following EMN volley occurred with a latency of 50–80 msec, the second EMN volley after the stimulus occurred at a variable delay that fell within the range of inter-EMN intervals governed by the intrinsic spontaneous electromotor command (*D*). *E–H,* A short latency response (latency, 5 msec) occurred when the delay was >60 msec. When the EMN trigger-stimulus interval was reduced, a motor response could still be evoked, but with a longer latency of ~20 msec (*E, middle trace*). The shortest EMN-to-stimulus interval, after which a response could be obtained to microstimulation at this site, was ~20 msec (*E, bottom trace, F*). When the stimulus failed to evoke either the 5 or the 20 msec latency EMN response, an EMN volley occurred at ~80 msec after the stimulus (*E, lower trace, F*). The second EMN volley after a stimulus again occurred at a rather fixed latency of 80–100 msec (*F, open diamonds*). The histogram in *G* shows a cumulated summary of EMN timing after the stimulus (first responses in *black*, second responses in *open bars*). The distribution of the intrinsic, spontaneous command of inter-EMN intervals for the recording period illustrated in *E–G* is shown in *H*.

and was only observed in the immediate post-command period. It is therefore probably a corollary discharge-driven phenomenon, although the exact anatomical connections involved have not yet been described. Again, it is likely that this input to PCN arrives via a collateral branch of BCA axons that pass close to PCN en route for the MCA, or that PCN receives afferent connections from other corollary discharge associated nuclei (Bell and von der Emde, 1995).

The functional role of PCN

It is argued above that the field potentials recorded in PCN do not reflect premotor activity in this nucleus. However, our results show that many neuronal elements in PCN fire sporadically or tonically over a large part of the EOD cycle, and it is probable that these are the PCN cells that project to CN. The origin of such spontaneous activity has not been explored, and we cannot conclude whether PCN units might have an intrinsic pacemaker function, in addition to integrating information afferent to the electromotor command chain. An increase in the firing frequency of tonically firing units, or the onset of sporadic firing in otherwise silent units, was frequently associated with the generation of an EMN volley. Glutamate iontophoresis also drove the EMN firing frequency, and this was probably a result of direct stimulation of PCN neurons. Similarly, electrosensory stimulation activated unit firing in PCN at the same time that it provoked an EMN volley. Thus, it is likely that

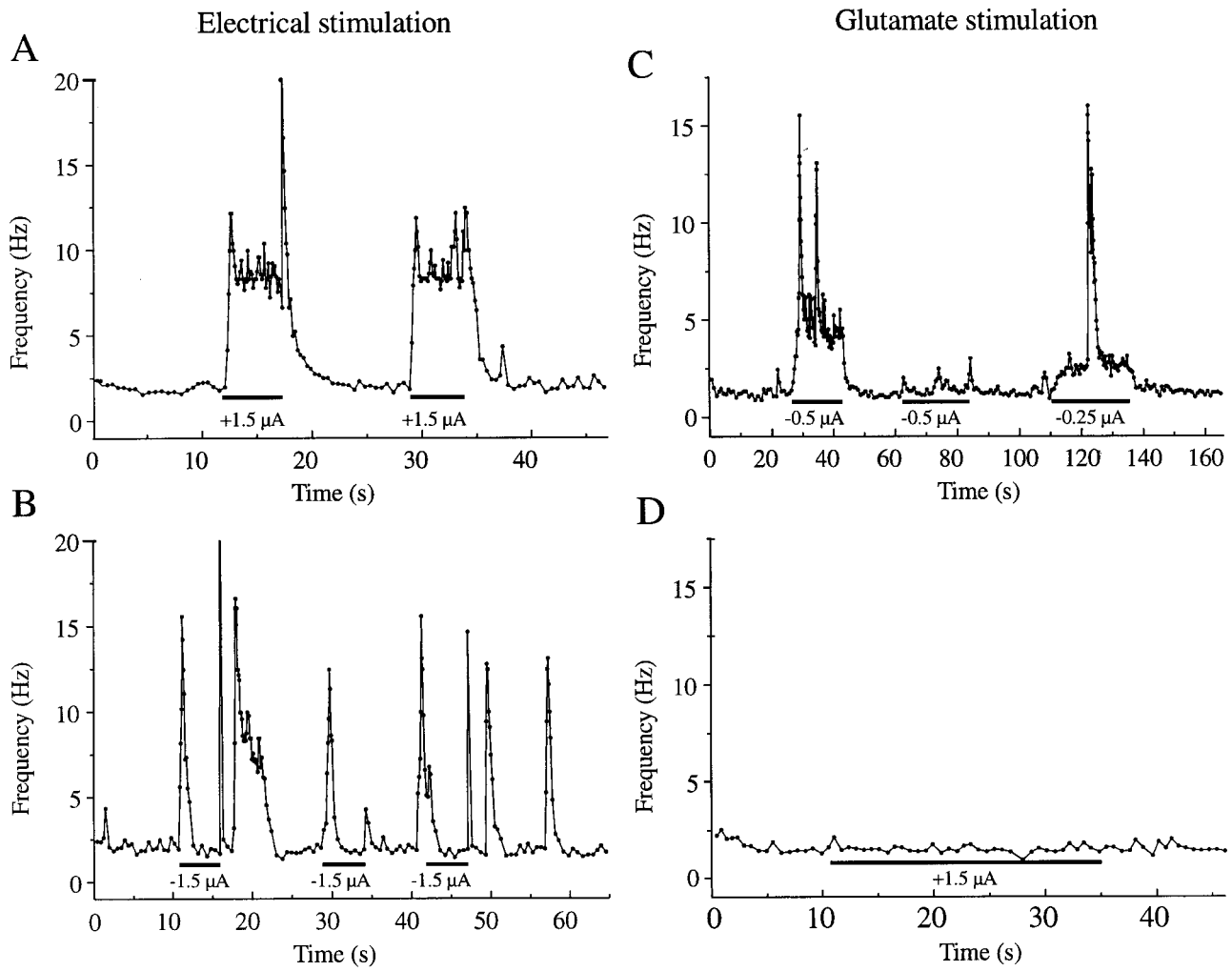

Figure 12. The effects of DC electrical stimulation and glutamate iontophoresis in PCN (2 different experiments). *A,* Electrical stimulation via the recording microelectrode, using constant current (1.5 μA) applied for several seconds, caused a tonic increase in EMN firing frequency when the electrode tip was positive. *B,* When the electrode tip was negative, the onset and termination of the stimulus pulse provoked a short-lasting phasic increase in EMN firing but no tonic response. *C,* Iontophoresis of L-glutamate (electrode tip negative, 0.5 μA) caused a tonic increase in EMN firing frequency, on which spontaneous momentary increases in firing rate could still be observed. The tonic level of the firing frequency depended on the amount of injection current. *D,* When the polarity of the iontophoretic current was inverted, no changes in EMN firing rate were evoked at this site.

PCN conveys many excitatory inputs to CN, although PCN neurons do not generally fire as a synchronized ensemble. We suggest that descending input from PCN is integrated at the postsynaptic level in CN. When the result of this integration process is sufficient to activate CN neurons beyond their firing threshold, initiation of the electromotor command and the subsequent firing of the entire electromotor pathway follows.

As discussed above, the most probable explanation for the timing of the first negative peak of the PCN field potential is that it is the result of backpropagation from CN. The functional role of such backpropagation is not clear, but we suggest that antidromic, synchronous invasion of the whole population of PCN output cells projecting to CN would serve as a potent resetting mechanism in the descending pathway.

The slow positive field potential associated with each electromotor event is probably the result of synchronous input to PCN provided by the corollary discharge-activated bursting units. The consequence of this input may be the generation of large IPSPs in PCN neurons. Somata of PCN cells are surrounded by large synaptic terminals that show strong anti-GAD immunoreactivity (Niso et al., 1989). Corollary discharge inhibition of PCN may act as a rate-limiting, and resetting, mechanism preventing the electromotor system from being driven too fast. Modulation of the inhibitory corollary discharge feedback to PCN may, in addition, play an important role in regulating the firing of the tonically and/or intrinsically sporadically active neurons and thus in the fine control of the length of the current inter-EOD cycle. However, the results show that the corollary discharge IPSP generated in PCN neurons does not alone decide the inter-EMN interval. Instead, the electromotor command rhythm probably depends on a regulated balance of excitatory and inhibitory modulation of distributed intrinsic pacemakers.

Comparison with electromotor pacemaker systems of other electric fish

Previous studies in gymnotiform electric fish (Heiligenberg et al., 1981, 1996; Kawasaki et al., 1988; Kawasaki and Heiligenberg, 1990; Keller et al., 1991; Metzner 1993) and in the wave-emitting mormyriform, *Gymnarchus niloticus* (Kawasaki and Heiligenberg, 1990; Kawasaki and Yuang-Xing, 1996), have identified similar prepacemaker nuclei (PPN) of their electromotor systems. In these fish, electromotor behavior is driven by the intrinsic regular rhythmic activity of the medullary pacemaker center. Descending pathways from PPN modulate this intrinsic pacemaker rhythm. In *Gymnarchus* and the pulse-emitting gymnotid *Hypopomus*, stimulation of PPN causes interruption of the EOD. In wave-type gymnotids, in which several subdivisions of the PPN have been described, different stereotyped modulations of the highly regular

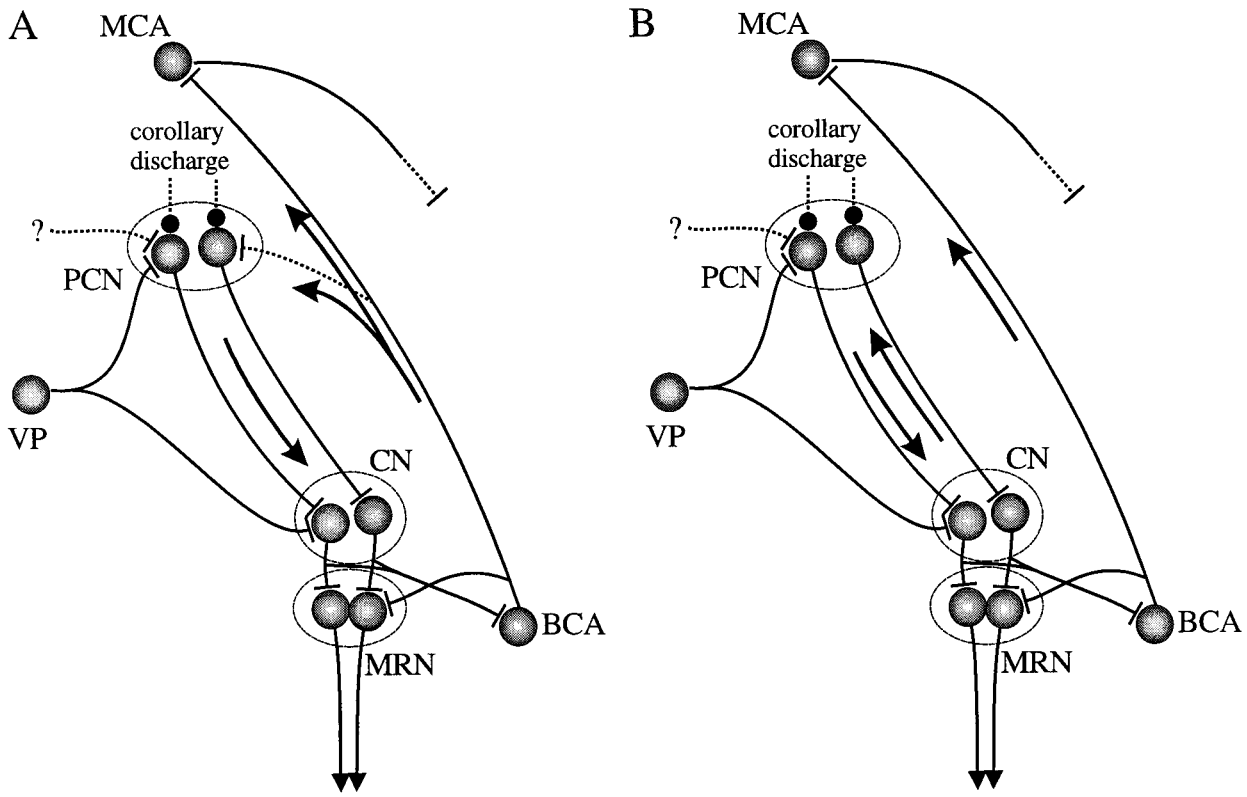

Figure 13. Possible schemes of functional connectivity to explain the genesis of electromotor-related events in PCN (see Discussion for explanation). In *A,* it is suggested that all motor-related events are the result of activity in the corollary discharge pathway; this would depend on the presence of an as-yet-undemonstrated collateral of BCA axons projecting toward the PCN. In *B,* it is suggested that the first negative motor-related field potential peak in PCN might be the result of antidromic invasion of PCN axons after generation of the electromotor command in CN. In both cases, nonsynchronized descending activity from PCN to CN is integrated by the electromotor command neurons in CN. *VP,* Ventroposterior nucleus of the torus semicircularis.

EOD emission have been attributed to activation of the individual neuronal subpopulations. It is possible that further detailed investigation of the precommand nucleus in *G. petersii* may reveal a similarly complex organization.

REFERENCES

Aljure E (1964) Neuronal control system of electric organ discharge in Mormyridae. PhD thesis, Columbia University.

Bass AH, Baker R (1997) Phenotypic specification of hindbrain rhombomeres and the origins of rhythmic circuitry in vertebrates. Brain Behav Evol 50:3–16.

Bauer R (1974) Electric organ discharge activity of resting and stimulated *Gnathonemus petersii* (Mormyridae). Behaviour 50:306–323.

Bauer R, Kramer B (1974) Agonistic behavior in mormyrid fish: latency-relationship between the electric organ discharges of *Gnathonemus petersii* and *Mormyrus rume.* Experientia 30:51–52.

Bell CC, von der Emde G (1995) Electric organ corollary discharge pathways in mormyrid fish. II. The medial juxtalobar nucleus. J Comp Physiol [A] 177:463–479.

Bell CC, Myers JP, Russell CJ (1974) Electric organ discharge patterns during dominance related behavioral displays in *Gnathonemus petersii* (Mormyridae). J Comp Physiol 92:201–228.

Bell CC, Finger T, Russell CJ (1981) Central connections of the posterior lateral line lobe in mormyrid fish. Exp Brain Res 42:9–22.

Bell CC, Libouban S, Szabo T (1983) Pathways of the electric organ discharge command and its corollary discharges in mormyrid fish. J Comp Neurol 216:327–338.

Bell CC, Dunn K, Hall C, Caputi A (1995) Electric organ corollary discharge pathways in mormyrid fish. I The mesencephalic command associated nucleus. J Comp Physiol [A] 177:449–462.

Bennett MVL, Pappas GD, Aljure E, Nakajima Y (1967) Physiology and ultrastructure of electrotonic junction. II. Spinal and medullary electromotor nuclei in mormyrid fish. J Neurophysiol 30:180–208.

Cohen AH, Guan L, Harris J, Jung R, Kiemel T (1996) Interaction between the caudal brainstem and the lamprey central pattern generator for locomotion. Neuroscience 74:1161–1173.

Clausse S (1985) Comparaison du centre initiateur de la comande motrice de la décharge électrique chez deux espèces de poissons, par une étude morpho-fonctionnelle. PhD thesis, Université de Paris VI.

Elekes K, Szabo T (1985) The mormyrid brainstem. III Ultrastructure and synaptic organization of the medullary "pacemaker" nucleus. J Neurosci 15:431–443.

Elekes K, Ravaille M, Bell CC, Libouban S, Szabo T (1985) The mormyrid brainstem. II. The medullary relay nucleus: an ultrastructural HRP study. J Neurosci 15:417–429.

Grant K, Bell CC, Clausse S, Ravaille M (1986) Morphology and physiology of the brainstem nuclei controlling the electric organ discharge in mormyrid fish. J Comp Neurol 245:514–530.

Grant K, von der Emde G, Gomez Sena L, Mohr C (1999) Neural command of electromotor output in mormyrids. J Exp Biol 202:1399–1407.

Grillner S, Georgopoulos AP (1996) Neural control. Curr Opin Neurobiol 6:741–743.

Grillner S, Deliagina T, Ekeberg O, el Manira A, Hill RH, Lansner A, Orlovsky GN, Wallen P (1995) Neural networks that co-ordinate locomotion and body orientation in lamprey. Trends Neurosci 18:270–279.

Heiligenberg W, Finger T, Matsubara J, Carr C (1981) Input to the medullary pacemaker nucleus in the weakly electric fish, *Eigenmannia* (sternopygidae, gymnotiformes). Brain Res 211:418–423.

Heiligenberg W, Metzner W, Wong CJH, Keller CH (1996) Motor control of the jamming avoidance response of *Apteronotus leptorhynchus*: evolutionary changes of a behavior and its neuronal substrates. J Comp Physiol [A] 179:653–674.

Hopkins CD (1988) Neuroethology of electric communication. Annu Rev Neurosci 11:497–535.

Katz PS (1995) Intrinsic and extrinsic neuromodulation of motor circuits. Curr Opin Neurobiol 5:799–808.

Kawasaki M, Heiligenberg W (1990) Different classes of glutamate receptors and GABA mediate distinct modulations of a neuronal oscillator, the medullary pacemaker of a gymnotiform electric fish. J Neurosci 10:3896–3904.

Kawasaki M, Yuang-Xing G (1996) Neuronal circuitry for comparison of timing in the electrosensory lateral line lobe of the African wave-type electric fish *Gymnarchus niloticus*. J Neurosci 16:380–391.

Kawasaki M, Maler L, Rose GJ, Heiligenberg W (1988) Anatomical and

functional organization of the prepacemaker nucleus in gymnotiform electric fish: the accommodation of two behaviors in one nucleus. J Comp Neurol 276:113–131.
Keller CH, Kawasaki M, Heiligenberg W (1991) The control of pacemaker modulations for social communication in the weakly electric fish *Sternopygus*. J Comp Physiol [A] 169:441–450.
Kramer B (1990) Electrocommunication in teleost fishes: behavior and experiments, p 240. Berlin: Springer.
Lissmann HW, Machin KE (1958) The mechanism of object location in *Gymnarchus niloticus* and similar fish. J Exp Biol 35:451–486.
Metzner W (1993) The jamming avoidance response in *Eigenmannia* is controlled by two separate motor pathways. J Neurosci 13:1862–1878.
Moller P (1970) "Communication" in weakly electric fish; *Gnathonemus niger* (Mormyridae). I. Variation of electric organ discharge (EOD) frequency elicited by controlled electric stimuli. Anim Behav 18:768–786.
Moller P, Serrier J, Bowling D (1989) Electric organ discharge display during social encounter in the weakly electric fish *Brienomyrus niger L.* (Mormyridae). Ethology 82:177–191.
Niso R, Serrier J, Grant K (1989) Mesencephalic control of the bulbar electromotor network in the mormyrid *Gnathonemus petersii*. Eur J Neurosci [Suppl] 2:176.
Szabo T (1957) Un noyau particulier dans la formation réticulé bulbaire de certains poissons électriques (mormyridés). Arch Anat Microsc Morphol Exp 46:81–92.
Serrier J (1982) Comportement électrique des mormyridé (Pisces). Electrogenèse en réponse à un signal exogène. Thèse d'Etat. Paris: Université Paris XI.
Serrier J, Moller P (1989) Patterns of electric organ discharge activity in the weakly electric fish *Brienomyrus niger L.* (Mormyridae). Exp Biol 48:235–244.
Teyssedre C, Boudinot M, Minisclou C (1987) Categorisation of interpulse intervals and stochastic analysis of discharge patterns in resting weakly electric fish (*Gnathonemus petersii*). Behaviour 102:264–282.
Toerring MJ, Moller P (1984) Locomotor and electric displays associated with electrolocation during exploratory behavior in Mormyrid fish. Behav Brain Res 12:291–306.
von der Emde G (1999) Active electrolocation of objects in weakly electric fish. J Exp Biol 202:1205–1215.